PROCEEDINGS, 49th Workshop on Geothermal Reservoir Engineering
Stanford University, Stanford, California, February 12-14, 2024
SGP-TR-227

# Developing High-Temperature Functional Microcapsules for Delayed Flow Diverter Formation in EGS Reservoirs

Chun Chang[1], Seiji Nakagawa[1], Oscar Olivarez Sandoval[2,1], William Kibikas[3], Timothy Kneafsey[1], Patrick Dobson[1], Abraham Samuel[4], Michael Otto[5], Stephen Bruce[5], Carlos Rodriguez[5], Nils Kaargeson-Loe[5], Robert Banker Comer[5]

[1]Lawrence Berkeley National Laboratory, Berkeley, CA 94720

[2]Contra Costa College, San Pablo, CA 94806

[3]Sandia National Laboratories, Albuquerque, NM 87185

[4]Geo Energize, LLC, La Quinta, CA 92253

[5]Baker Hughes Inc., Houston, Texas

[*]Corresponding author: chunchang@lbl.gov

**Keywords:** Enhanced Geothermal System; Fracture permeability manipulation; Flow diverter; Microcapsules; Microfluidics

## ABSTRACT

During Enhanced Geothermal System development, subsurface permeability is enhanced via stimulation processes that re-open pre-existing fractures, create new ones, or achieve a combination of both. Because of the heterogeneous nature of fractures, some fractures or portions of a fracture will take more flow than others, leading to fast fluid flow and a rapid decline of heat production. While near-wellbore fluid flow management has been widely investigated, controlling the reservoir permeability away from wells is challenging, as injected materials need to form solid plugs only after they reach the target locations. To control the timing of the flow-diverter formation in high temperature conditions, we are developing a technology to deliver one or more components of the diverter-forming chemicals in microcapsules with a thin polymer shell. The material properties of the shell are designed so that it can withstand moderately high temperatures (up to 200˚C) of the injected fluid for a short period of time (up to 1 hour), but thermally degrades and releases the reactants at higher reservoir temperatures. A microfluidic system has been developed that can continuously produce reactant-encapsulating particles. The diameter of the produced particles is in the range of ~250-650 μm, which can be controlled by using capillary tubes with different diameters and by adjusting the flow rates of the encapsulated fluid and the UV-curable epoxy resin for the shell. Laboratory experiments have demonstrated that (1) microcapsules containing chemical activators can be produced at different sizes and geometries, (2) the durability of the shell can be produced and tuned to satisfy different conditions, and (3) the microcapsules release their contents at high-temperatures, thus achieving their intended role in activator release and flow-diverter formation. SAND2023-10370A.

## 1. INTRODUCTION

An enhanced geothermal system (EGS) typically involves a reservoir stimulation process that re-opens pre-existing fractures, creates new ones, or achieves a combination of both. Ideally these newly created, highly conductive conduits provide pathways for water to circulate throughout the stimulated rock volume, and increased water-rock contact areas for heat exchange. However, even when a well-distributed flow network is created successfully, because of the heterogeneous fracture properties including geometry, aperture, connectivity, and their time-dependent evolution, some fractures or portions of a fracture will take more flow than others (Figure 1a). This potentially leads to heat extraction from only a small portion of the reservoir (known as "short circuiting"), resulting in rapid thermal decline of the heat extraction fluid (Doe and McLaren, 2016). The DOE Geothermal Technologies Office recently sponsored a comprehensive modeling study to evaluate the viability of EGS (Kennedy et al., 2021: Doe et al., 2022). One of the major conclusions of this study was that the stimulated fracture network will "require an active management approach that shuts down the more permeable pathways as they experience thermal breakthrough at the production well." High permeability fractures connecting injection and production wells serve as fast flow paths that would function as undesired short circuits, leading to premature thermal breakthrough. High permeability fractures could also contribute to large fluid losses from the EGS reservoir, as was observed at the Hijiori test site (Tester et al., 2006), making it difficult to sustain its operation. For developing a sustainable and economical EGS, it is critical to control the fluid flow within a created reservoir and optimize the subsurface heat exchange performance in stimulated fractures.

Currently, standard approaches for altering reservoir fluid flow target the near-wellbore environment, including a variety of well completion and zonal isolation methods by which fluid flow into or out of a well is controlled. For instance, the application of different lost circulation materials has shown promise in efficiently plugging wellbore fractures to eliminate loss of drilling fluids while drilling (Pu et al., 2022; Kibikas et al., 2023; Nakagawa et al., 2023a). Short-term flow diverter plugs that thermally degrade have been developed and used to facilitate multizonal stimulation of EGS wells (e.g., Petty et al., 2011; Nordin et al., 2013). A variety of well completion and zonal isolation methods has also been applied, by which fluid flow into or out of a well is controlled. While management of near-wellbore fluid flow is critically important for maintaining fluid production from EGS reservoirs, it has limited impact in controlling the fluid flow away from the wells, which is necessary for optimization of heat recovery and reservoir performance.

The focus of this study is to reduce and manage the permeability of fast flow paths within an EGS reservoir far away from both injection and production wells, achieving distributed flow and heat exchange within a larger reservoir volume (Figure 1b). To control the timing of the flow-diverter formation in high temperature conditions, we are developing a technology that involves (1) microparticles (capsules) containing the reactants ("encapsulated microparticles"), for delaying the diverter-forming reactions until the particles are transported to

a desired reservoir location, by optimizing the capsule's shell properties, and (2) silica-gel and metal-silicate-based flow diverters that are stable under EGS conditions and can be dissolved and disintegrated when needed. The controlled reaction of the diverter-forming components is made possible primarily by thermal degradation of the particle's polymer shells, which requires the understanding of the degradation (or triggering) and transport characteristics of the reactant-delivering microcapsules.

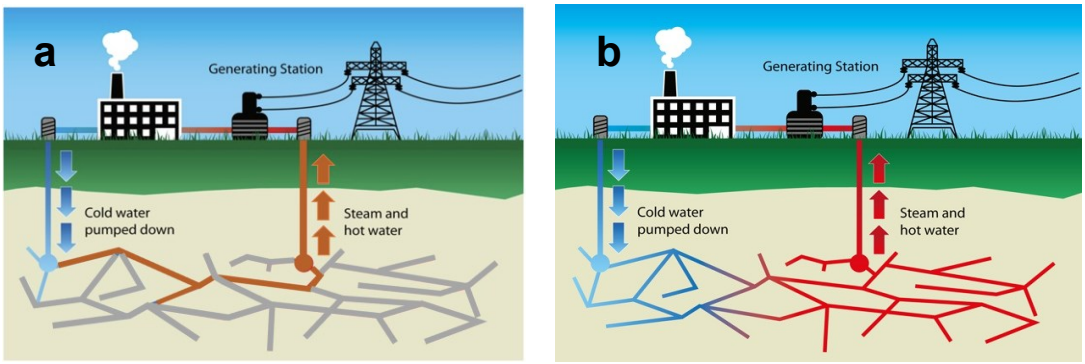


**Figure 1: The objective of this study is to develop a technology for reducing fast flow paths consisting of highly permeable fractures in (a) by creating more distributed paths occupying a larger reservoir volume (b) at locations away from both injection and production wells in EGS reservoir (Revised from https://courses.cit.cornell.edu/mclaskey/vib/earth/KatieWhite/geothermal.html).**

## 2. MATERIALS AND METHOD

### 2.1 Silicate-gel-based flow diverter

This research uses silicate-gel-based flow diverters at elevated temeraptures. The precursor used in this study is sodium silicate, which starts the gelation reaction in the presence of acid activators (e.g., An-Peng, 1963; Bauer et al., 2004). The acid activators could be either strong acids (e.g., HCl, $H_2SO_4$, $HNO_3$) or weak acids such as acetic acid, citric acid and formic acid. When acid activators are delivered via microcapsules, the total amount of the acid that can be delivered to the target location would be limited by the volume and concentration of the particles in the injected fluid. This makes it necessary to use highly concentrated acid. Weak, organic acids are preferable for keeping the pH at a safe, acceptable level, while providing the necessary amount of $H^+$, as long as the strength and durability of the gel is sufficient. When organic weak acids are used, however, their temperature stability under the EGS conditions needs to be considered. In this research, we selected acetic acid, since it has been shown to be stable up to ~230°C for 72 hours (Li et al., 2017). The reaction between sodium silicate and acetic acid can be summarized as follows:

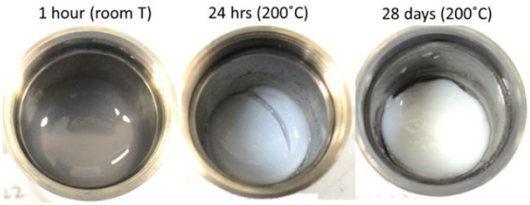


**Figure 2: Photo images of the gels produced by mixing sodium silicate (10 wt%) and acetic acid (4.6 wt%) (Revised from Nakagawa et al., 2023b).**

$$(Na_2O)_x(SiO_2)_{y(liquid)} + 2xCH_3COOH_{(liquid)} \rightarrow (SiO_2)_{y(solid)} + 2xCH_3COONa_{(liquid)} + xH_2O \qquad \text{Eq. (1)}$$

Previously, we conducted a series of laboratory experiments by mixing sodium silicate with different concentrations of acetic acid. Stability of the produced gels and precipitates was tested after heating at 200 ˚C for ~72 hours (short-term tests) and up to 28 days (long-term tests). Results from these experiments indicate that a combination of high-concentration sodium silicate (10 wt.%) and acetic acid (4.6 wt.%) produces a high-water-content silica gel that is stable under a high-temperature, closed (no-flow) environment (Figure 2 and Nakagawa et al., 2023b).

### 2.2 Microcapsules production by single-step microfluidic encapsulation

The diverter-delivering particles (capsules) need to be sufficiently small, so that they can be injected into reservoir fractures acting as fast paths (currently apertures of ~0.5 mm and larger are targeted). Also, the particles need to have a very thin shell, maximizing the amount of the encapsulated chemical. Such particles also need to be produced in a large quantity, efficiently and economically. To meet these requirements, we used the single-step microfluidic encapsulation method for producing diverter-encapsulating microparticles. Among several possible techniques for implementing this method, we adopted a three-phase glass capillary device, which is a promising technique for generating microcapsules with well-controlled geometry (Arriaga et al., 2015; Nabavi et al., 2015). The technique is based on a combined co-flow and counter-current flow in a glass capillary device (Figure 3a). The microcapsules are then produced through a flow focusing mechanism in which fluids containing core and shell materials are forced through a narrow junction. In addition to the core and shell fluid flow, the system involves an outer carrier fluid flow. The capillary junction simultaneously pinches off the interior core and exterior shell fluids, forming a double-layer droplet suspended in the outer carrier fluid (as shown in Figure 3a). The carrier fluid is used to stabilize the droplets. Once the double-layer droplets are formed, the outer shell, consisting of a photopolymer material, is photopolymerized by UV light to form the microcapsule. Compared to the conventional two-step microfluidic encapsulation approach (e.g., Okushima et al., 2004; Kim et al., 2011), the advantages of the single-step microfluidic encapsulation are (1) the easy control of

individual flow rates, because the flow rates of the inner and middle fluid do not need to be synchronized; (2) the capability to generate very thinly shelled particles; (3) the simpler system design and smaller number of capillaries and connectors, which makes fabrication of the production system easier than the device composed of two sequential drop generation units.

After a systematic evaluation of the polymer shell materials that could be potentially used for geothermal applications, NOA 61 UV-curable epoxy (Norland Products, NJ) was selected for its low viscosity, fast UV curing time, and most importantly, high temperature stability. The two core materials that we used in our investigation are water stained with a fluorescent tracer dye, and acetic acid (10-50 wt.%) stained with blue food dye. The carrier fluids were either silicone oil or mineral oil with a lower viscosity. During production, the particle size and shell thickness were changed by controlling the relative magnitudes of viscous, capillary and inertial forces of the three fluids used in the microfluidic device. Figure 3b is a photograph of the production system that involves three syringe pumps for core, shell and carrier fluid injection, and a UV lamp installed in-situ to cure the epoxy shell in the collection tube. We injected the carrier fluid (Mineral oil, Gamsol) at a constant flow rate of 300 μL/min, and injected core liquid (50 wt.% acetic acid) and shell epoxy (NOA61) at different rates, ranging from 3 to 15 μL/min.

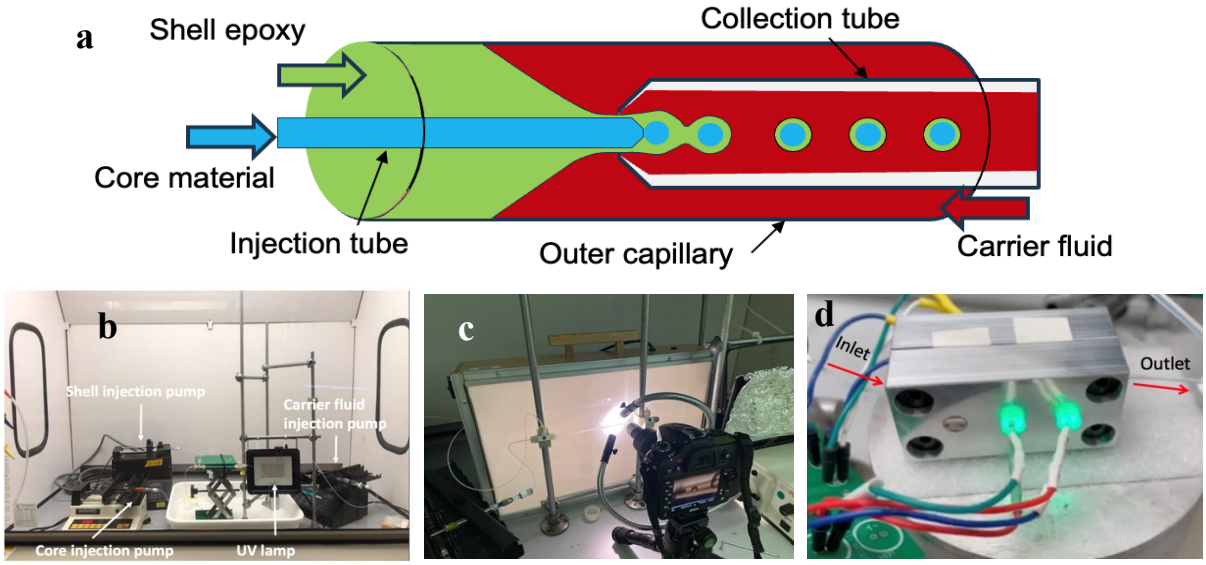


**Figure 3: (a) Schematic of the microfluidic device for producing microcapsules. (b) Photograph of the production system developed at Berkeley Lab. (c-d) Photographs of the microscope imaging system and the LED-based particle tracking device.**

We also developed a microscope imaging system and a LED-based particle tracking device to provide direct visualization of the particle forming mechanism and automatically collect production information, e.g., the production rate. Figures 3c and d are photos of the imaging system and LED-based particle tracking device. During production, the flow of microparticles will induce light intensity changes in the aluminum block, which will be converted into electrical signal and recorded.

### 2.3 Hydrothermal experiments

In this study, hydrothermal experiments were conducted using the produced microcapsules and sodium silicate solutions to investigate the thermal degradation behavior of microcapsules and control of silica gel plug formation. The primary equipment used in this research is a series of small, stainless-steel Parr reactor vessels (Figure 4), containing small, sealable internal cells made of corrosion-resistant grade-2 titanium with high-temperature Viton O-rings (rated for 230°C) (e.g., Nakagawa et al., 2022). We demonstrated that the system could contain water vapor at 200°C without any fluid loss over 1 month, which is important for maintaining constant reaction environment and simulating EGS conditions.


**Figure 4: Equipment used for hydrothermal experiments involving produced microcapsules and sodium silicate solutions. To minimize fluid loss and chemical contamination of the samples, sealable internal cells (a) were used in combination with small Parr reactor vessels (b). These vessels were heated in a convection oven at 150-200 °C (From Nakagawa et al., 2023b).**

## 3. RESULTS AND DISCUSSION

### 3.1 Dynamics of acetic acid (core)-epoxy (shell) double emulsion formation

Figure 5a depicts representative time-lapse images showing the formation of a microcapsule in the capillary device. As the acetic acid (50 wt.%) and epoxy were co-injected from the left boundary via the injection tube and the outer capillary tube, a double layer ganglion formed at the tip of the injection tube. At the same time, the injection of carrier fluid induced elongation of the ganglion by viscous dragging force until 0.2s when snap-off of the ganglion occurred and the double-layer ganglion pinched off from the injection tube. The flow of the microcapsules in the collection tube were recorded by the LED-based tracking device, and Figure 5b shows the converted electrical signals over 2s. The spike of the voltage indicates passing of a microcapsule at a signal-to-noise ratio of > 40. Although we have not conducted a detailed analysis yet, potentially the shape of each spike can also be used to characterize the particle shape parameters (e.g. particle size, core-shell diameter ratio). Combining these two systems can produce a unique dataset for understanding the dynamics of microcapsule formation, and allow automatic monitoring of the performance during production.

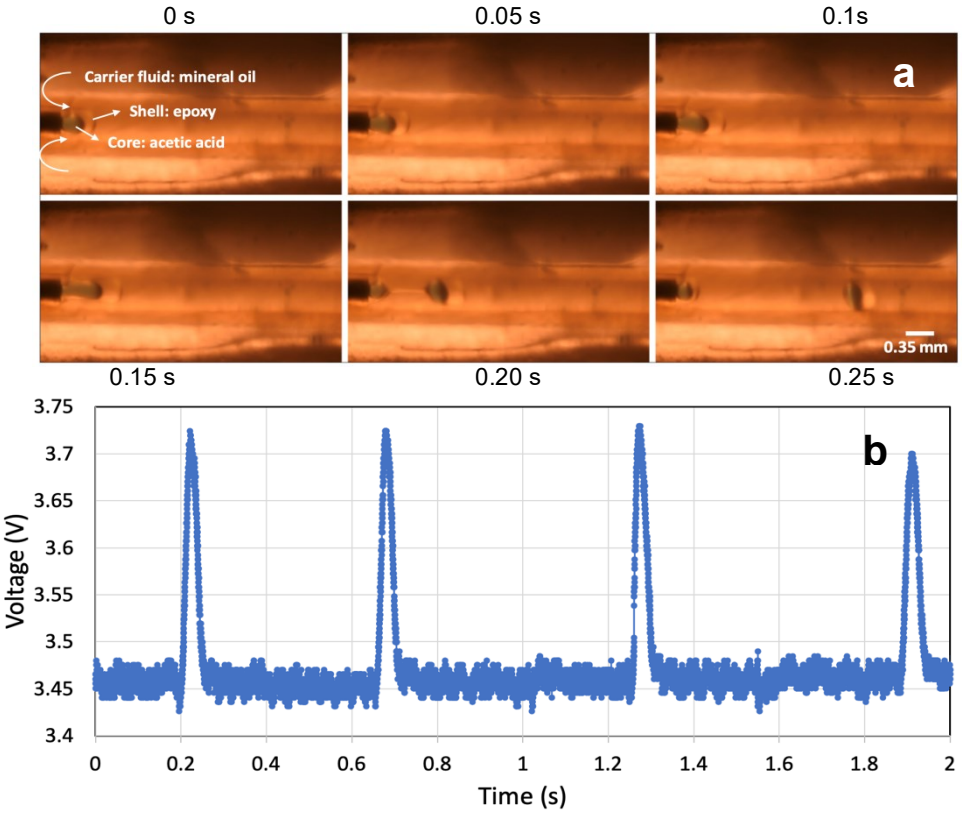


**Figure 5: (a) Time-lapse images showing the formation of microcapsules by the microfluidic system at a core injection rate of 3 µl/min, shell injection rate of 15 µL/min, and a carrier fluid injection rate of 300 µL/min. (b) Changes of the electrical signal in the collection tube captured by the LED-based particle tracking device**

### 3.2. Characterization of produced microcapsules

Figures 6a and b show microscope images of some of the produced microcapsules with sizes <500 µm. Figure 6c presents the measured microcapsule diameters and core diameters, and Figure 6d depicts the density measured from randomly selected individual microcapsules. The average capsule and core diameters are 458 ± 23 µm and 290 ± 22 µm, respectively, and the average density is 1.18 ± 0.095 g/cm$^3$. The statistics of diameter and density measurements on microcapsules indicate the consistency of the products and high-quality control of the production system.

We also confirmed the capability of the microfluidic system in producing microcapsules with a range of sizes and core materials by adjusting the tube sizes and fluid injection rates. For instance, Figure 7 shows example microscope images of more products, including (a) water stained with fluorescent tracer dye, (b) 10 wt.% acetic acid solution and (c-d) 50% acetic acid solution stained with blue food dye. Figure 7 also illustrates the capability in producing microcapsules with a particle diameter of ~250 to 650 µm and a core diameter of ~220 to 540 µm. After being UV cured and dried, the microcapsules were tested under elevated temperature and pressure relevant to EGS conditions.

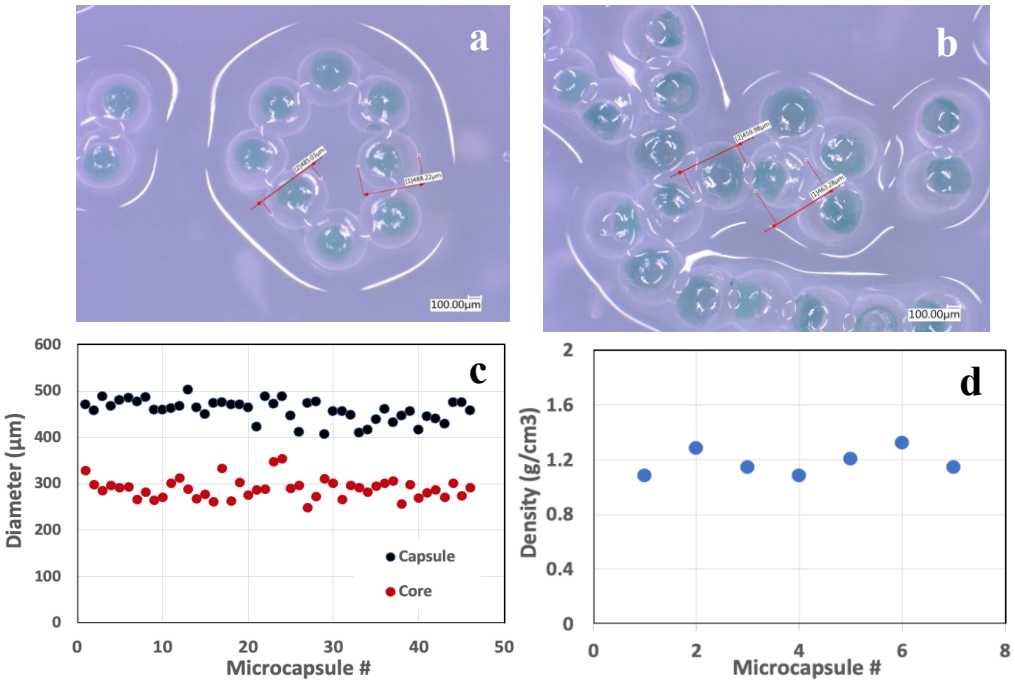


**Figure 6: (a, b) Example microscope images showing the produced microcapsules at <500 µm diameter. (c) Diameter distribution of microcapsules and cores measured from representative microcapsules. (d) Density distributions measured from individual microcapsules.**

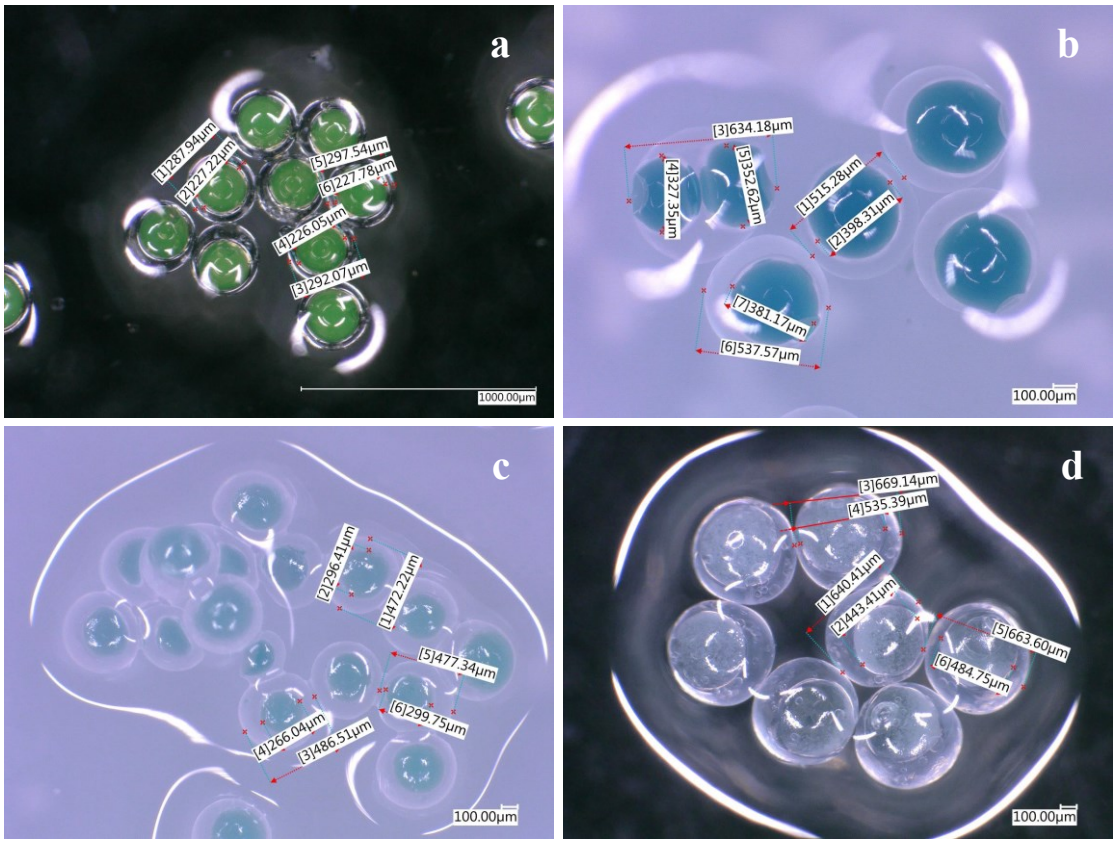


**Figure 7: Microscope images showing produced microcapsules with a variety of characteristics, including (a) water core stained with fluorescent dye, (b) 10 wt.% acetic acid core stained with blue food dye, and (c, d) 50 wt.% acetic acid core stained with blue food dye with a range of particle sizes.**

**3.3 Silicate gel plug formation delayed by microcapsules under elevated temperatures**

By using the microcapsules in Figure 6, we conducted hydrothermal experiments with 10 wt.% sodium silicate at 150-200°C (Figure 8a). Figure 8b demonstrates the thermal stability of produced microcapsules after 1.5 h heating at 150 °C. For this sample, heating of the system was resumed and continued under 200°C for another 30 min. Figure 8c shows the result, indicating partial degradation of the microcapsules but no considerable gel formation. In contrast, Figure 8d presents another experiment that shows degradation of most of the microcapsules when subjected to heating at 150°C for 1.5 hours followed by 200°C for 1.5 hours. Again, no considerable gel formation was observed, and this is probably due to an insufficient amount of acetic acid for gelation reaction. Figure 8e and f are microscope images showing the detailed geometry of the microcapsules after the hydrothermal experiments, with breached shell and geometry of remaining microcapsules.

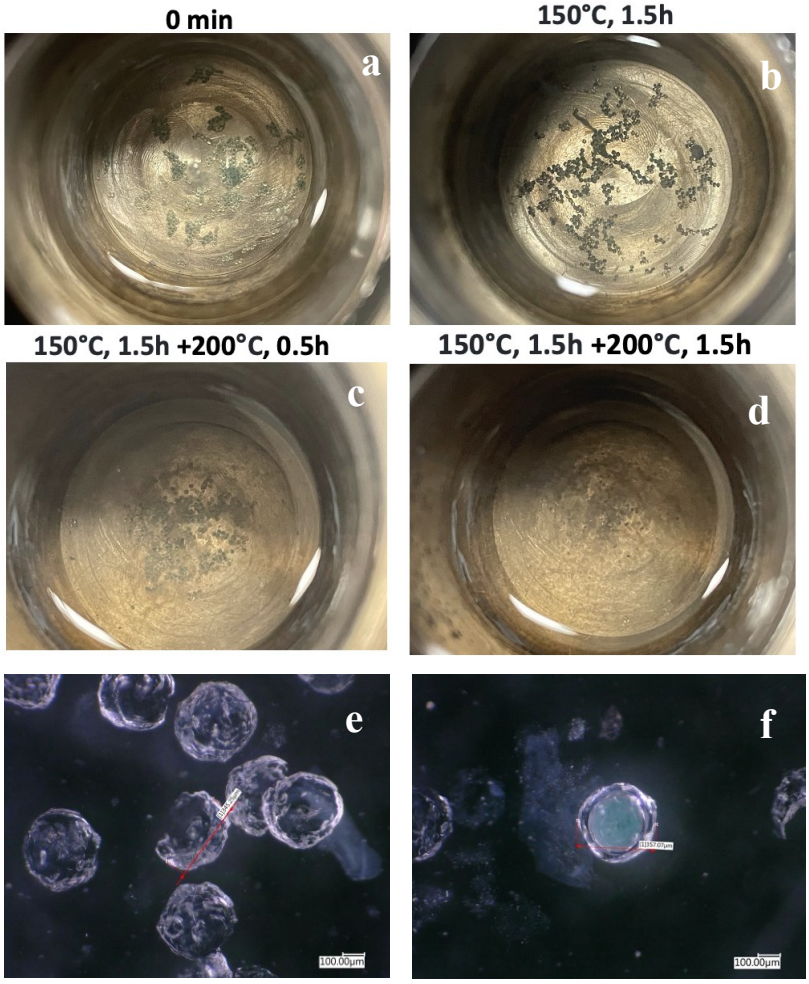


**Figure 8: (a-d) Photograph of the hydrothermal tests on acetic acid (50 wt.%) encapsulated microparticles with 10 wt.% sodium silicate at 150-200 °C.(e) Microscope images of the microcapsules after shell breach. (f) Microscope image of a remaining microcapsule.**

We also conducted hydrothermal experiments on the produced microcapsules with larger sizes which provide more acetic acid for gelation reaction. Figure 9a and b are microscope and SEM images of the investigated microcapsules at a diameter of ~650 µm and core size at ~450 µm. A higher concentration of sodium silicate (40 wt.%) was also applied in the hydrothermal experiments (Figure 9c). Figures 9d demonstrates the stability of microcapsules after 30 min heating at 150 °C, indicating the epoxy shell successfully isolated and protected the core reactant (50 wt.% acetic acid) from the sodium silicate solution for at least 30 min at 150°C. With this sample, heating of the system was resumed and continued at 150°C for another 1 hour after the observation. As shown in Figures 9e and f, the degradation and breach of the epoxy shell released acetic acid and initiated reaction with the surrounding sodium silicate solution, forming an intact gel plug with a length up to 2.0 cm. Microscope images of the gel plug clearly showed the degradation of microcapsules, leaving a semi-spherical shell structure within the plug (Figures 9g, h).

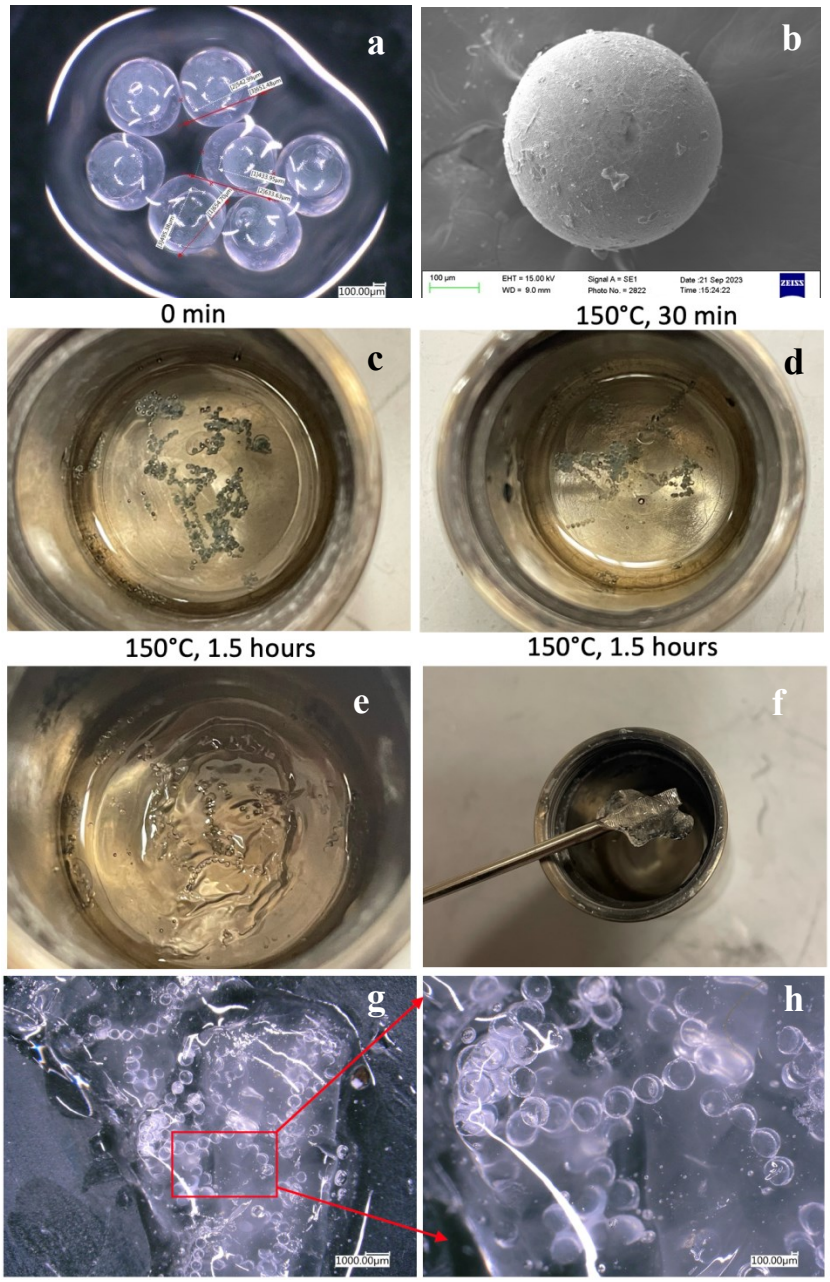


**Figure 9: (a) Microscope and (b) SEM images of the produced microcapsule at 650 µm. (c-f) Photograph of the hydrothermal tests using acetic acid (50 wt.%) encapsulated microcapsules with 40 wt.% sodium silicate at 150°C. (e-f) Microscope images of the silica gel plug after shell breach.**

## 4. CONCLUSIONS

We successfully developed a microfluidic system and produced reactant-encapsulating microcapsules for EGS fracture manipulation. We also built an in-situ imaging and particle tracking system to understand the encapsulation process and automatically monitor and assess the particle production performance. We demonstrated the capability of the system for producing microcapsules containing different types of flow-diverter-forming reactants, with sizes ranging from ~250 to 650 µm and shell thickness from 30 to 80 µm. We also conducted hydrothermal experiments at temperatures between 150-200°C on the produced microcapsules, confirming that (1) the reactions were delayed by 0.5-1 hours and that (2) once triggered, reaction can be enhanced by the increased reactive interfacial areas and reduced diffusion length. These properties of reactant-encapsulating microcapsules are critically important for delivering gel-forming chemicals away from the injection wells, delaying the reaction kinetics, and then achieving the objective of manipulating EGS reservoir fracture permeability. Further work will be conducted to test the thermal degradation and delayed silicate gel and metal precipitate forming performance of the microcapsule for a range of activator core materials, particle sizes, shell thickness and concentrations. Additionally, the current microfluidic system will be scaled up so that a large quantity of the microcapsules can be produced rapidly.

**ACKNOWLEDGMENTS**

This work is supported by the U.S. Department of Energy, Office of Energy Efficiency and Renewable Energy (EERE), Office of Technology Development, Geothermal Technologies Office, under Award Number DE-AC02–05CH11231 with LBNL and contract DE-NA0003525 with SNL. Sandia National Laboratories is a multi-mission laboratory managed and operated by National Technology & Engineering Solutions of Sandia, LLC, a wholly owned subsidiary of Honeywell International Inc., for the U.S. Department of Energy's National Nuclear Security Administration. This paper describes objective technical results and analysis. Any subjective views or opinions that might be expressed in the paper do not necessarily represent the views of the U.S. Department of Energy or the United States Government.

**REFERENCES**

An-Peng, T.: A theory for polymerization of silica acid, Sci. Sin, 9(13111320), (1963), 15.

Arriaga, L.R., Amstad, E., and Weitz, D.A.: Scalable single-step microfluidic production of single-core double emulsions with ultra-thin shells, Lab Chip, 15, (2015), 3335.

Bauer, S., Galbreath, D., Hamilton, J., and Mansure, A.: Comments on high temperature plugs: Progress report on polymers and silicates, GRC Transactions, 28 (2004), 145-152.

Doe, T., and McLaren, R.: Discrete Fracture Network Analysis of Controlling Factors for EGS Performance, PROCEEDINGS, 41st Workshop on Geothermal Reservoir Engineering, Stanford University, Stanford, CA, February 22-24, SGP-TR-209, (2016).

Doe, T., Riahi, A., Fu, P., Damjanac, B., Sonnenthal, E., Finnila, A., Kennedy, B.M., and Blankenship, D.: Performance evaluation of engineered geothermal systems using discrete fracture network simulations, Proceedings, 47th Workshop on Geothermal Reservoir Engineering, Stanford University, Stanford, CA Feb. 7-9 (2022), SGP-TR-223.

Kennedy, B.M., Blankenship, D., and Doe, T., et al.: Performance Evaluation of Engineered Geothermal Systems Using Discrete Fracture Network Simulations, Lawrence Berkeley National Laboratory Report, (2021), https://escholarship.org/uc/item/4168d73x.

Kibikas, W., Chang, C., Bauer, S.J., Nakagawa, S., Dobson, P., Kneafsey, T., and Samuel, A.: Thermal degradation and mixture properties of materials used for lost circulation management, PROCEEDINGS, 48th Workshop on Geothermal Reservoir Engineering, Stanford University, Stanford, California, February 6-8, (2023), SGP-TR-224.

Kim, S.H., and Weitz, D.A.: One-step emulsification of multiple concentric shells with capillary microfluidic devices, Angew. Chem. Int. Ed. Engl., 123, (2011), 8890–8893.

Li, Y., Zhou, S., Li, J., Ma, Y., Chen, K., Wu, Y., and Zhang, Y.: Experimental study of the decomposition of acetic acid under conditions relevant to deep reservoirs, Applied Geochemistry, 84, (2017), 306-313.

Nabavi, S.A., Vladisavljević, G.T., Gu, S., and Ekanem, E.E.: Double emulsion production in glass capillary microfluidic device: parametric investigation of droplet generation behavior, Chem. Eng. Sci., 130, (2015), 183-196.

Nakagawa, S., Chang, C., Kibikas, W., Kneafsey, T.J., Dobson, P., Samuel, A. and Bauer, S.J.: Laboratory Evaluation of the Short-Term Clogging Behavior of Various Materials and Their Combined Use for Lost Circulation Management. PROCEEDINGS, 48th Workshop on Geothermal Reservoir Engineering Stanford University, Stanford, CA, February 6-8, (2023a), SGP-TR-224.

Nakagawa, S., Kibikas, W., Chang, C., Kneafsey, T.J., Dobson, P., Samuel, A., Otto, M., Bruce, S., Kaargeson-Loe, N., and Bauer, S.J.: Stability and Breakdown of Acid- Induced Hydrated Silicate Gels and Metal Silicate Hydrates under Geothermal Conditions: A Preliminary Laboratory Study. PROCEEDINGS, 48th Workshop on Geothermal Reservoir Engineering Stanford University, Stanford, CA, February 6-8, (2023b), SGP-TR-224.

Nordin, Y., Petty, S., Cladouhos, T., Swyer, M., and DeRocher, T.: Multiple zone geothermal stimulation case study: Fluid diversion using thermo-degradable zonal isolatin materials, GRC Transactions, 37, (2013), 51-55.

Okushima, S., Nisisako, T., Torii, T., and Higuchi, T.: Controlled production of monodisperse double emulsions by two-step droplet break up in microfluidic devices, Langmuir, 20, (2004), 9905–9908.

Pu, L., Xu, P., Xu, M.B., Song, J.J. and He, M: Lost circulation materials for deep and ultra- deep wells: a review. J. Pet. Sci. Eng. 214, (2022), 110404. Petty, S., Bour, D., Nordin, Y., and Nofziger, L.: Fluid diversion in an open-hole slotted liner – a first step in multiple zone EGS stimulation, Proceedings, 36th Workshop on Geothermal Reservoir Engineering, Stanford University, Stanford, CA, Jan. 31 – Feb. 2, (2011), SGP-TR-191.

Petty, S., Bour, D., Nordin, Y., and Nofziger, L.: Fluid diversion in an open-hole slotted liner – a first step in multiple zone EGS stimulation, Proceedings, 36th Workshop on Geothermal Reservoir Engineering, Stanford University, Stanford, CA, Jan. 31 – Feb. 2, (2011), SGP-TR-191.

Tester, J.W., Anderson, B.J., Batchelor, A.S., Blackwell, D.D., DiPippo, R., Drake, E.M., Garnish, J., Livesay, B., Moore, M.C., Nichols, K., Petty, S., Toksoz, M.N., and Veatch, R.W: The Future of Geothermal Energy: Impact of Enhanced Geothermal Systems (EGS) on the United States in the 21st Century, Massachusetts Institute of Technology, (2006), Cambridge, MA, INL/EXT-06-11746.